ACS Synthetic Biology

pubs.acs.org/synthbio

Research Article

Quantification of Genome Editing and Transcriptional Control Capabilities Reveals Hierarchies among Diverse CRISPR/Cas Systems in Human Cells

Mario Escobar, Jing Li, Aditi Patel, Shizhe Liu, Qi Xu, and Isaac B. Hilton*

Cite This: *ACS Synth. Biol.* 2022, 11, 3239–3250

Read Online

ACCESS | Metrics & More | Article Recommendations | Supporting Information

ABSTRACT: CRISPR/Cas technologies have revolutionized the ability to redesign genomic information and tailor endogenous gene expression. Nevertheless, the discovery and development of new CRISPR/Cas systems has resulted in a lack of clarity surrounding the relative efficacies among these technologies in human cells. This deficit makes the optimal selection of CRISPR/Cas technologies in human cells unnecessarily challenging, which in turn hampers their adoption, and thus ultimately limits their utility. Here, we designed a series of endogenous testbed systems to methodically quantify and compare the genome editing, CRISPRi, and CRISPRa capabilities among 10 different natural and engineered Cas protein variants spanning Type II and Type V CRISPR/Cas families. We show that although all Cas protein variants are capable of genome editing and transcriptional control in human cells, hierarchies exist, particularly for genome editing and CRISPRa applications, wherein Cas9 ≥ Cas12a > Cas12e/Cas12j. Our findings also highlight the utility of our modular testbed platforms to rapidly and systematically quantify the functionality of practically any natural or engineered genomic-targeting Cas protein in human cells.

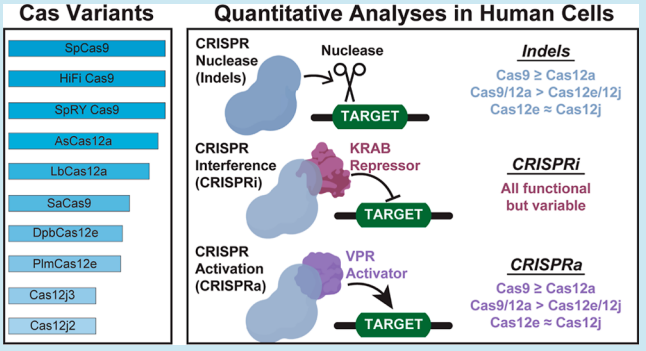

KEYWORDS: *genome editing, CRISPR/Cas systems, gene regulation, CRISPRa, CRISPRi*

INTRODUCTION

Significant phylogenetic and functional diversity has recently been uncovered among CRISPR/Cas systems.[1,2] Remarkably, components from at least 6 different CRISPR/Cas families (Cas9, Cas12a, Cas12b, Cas12e, Cas12f, and Cas12j) have been identified that enable editing of mammalian genomes, transcriptomes, and/or epigenomes[3−11] (Figure S1). Although the Type II CRISPR/Cas system identified in *Streptococcus pyogenes* (SpCas9) is the most well-characterized and widely used system for genome editing,[3−5] CRISPR activation (CRISPRa), and CRISPR interference (CRISPRi) in mammalian cells,[12−19] the relatively large size of SpCas9, the NGG PAM sequence requirements, and the potential for off-target effects can restrict the utility of SpCas9 in some contexts.[20−22]

To overcome these limitations, engineered variants of SpCas9 with increased fidelity, such as hypoCas9,[23] eSpCas9,[24] and HiFi Cas9,[25] have been developed for use in mammalian cells. Additionally, SpCas9 variants with altered PAM specificities, such as SpRYCas9,[26] VQR SpCas9 and EQR SpCas9,[27] SpCas9-NG,[28] and xCas9,[29] have been created. Furthermore, natural Cas9 orthologues, such as *Staphylococcus aureus* Cas9 (SaCas9);[30] *Neisseria meningitidis* Cas9 (NmCas9);[31,32] and *Campylobacter jejuni* Cas9 (CjCas9),[33] have been characterized that have smaller sizes and different PAM requirements than SpCas9, yet still retain robust activity in mammalian cells. CRISPR/Cas systems from the Type V family, such as Cas12a[6] (also called Cpf1), Cas12e[7] (also called CasX), and Cas12j[9] (also called CasΦ), have also been adopted for use in mammalian cells. Unlike Type II CRISPR/Cas family members, Cas proteins associated with Type V CRISPR/Cas systems contain a single nuclease domain, require a T-rich PAM,[34] and typically have smaller sizes than SpCas9.

Although multiple CRISPR/Cas systems have been identified and tested in mammalian cells, differing PAM sequence requirements and the lack of isogenic expression vectors has made direct, systematic comparisons among genome editing and transcriptional modulatory (i.e., CRISPRa/CRISPRi) activities in mammalian cells challenging. Additionally, for many of the newly identified CRISPR/Cas

Received: March 28, 2022
Published: September 26, 2022

https://doi.org/10.1021/acssynbio.2c00156
ACS Synth. Biol. 2022, 11, 3239−3250

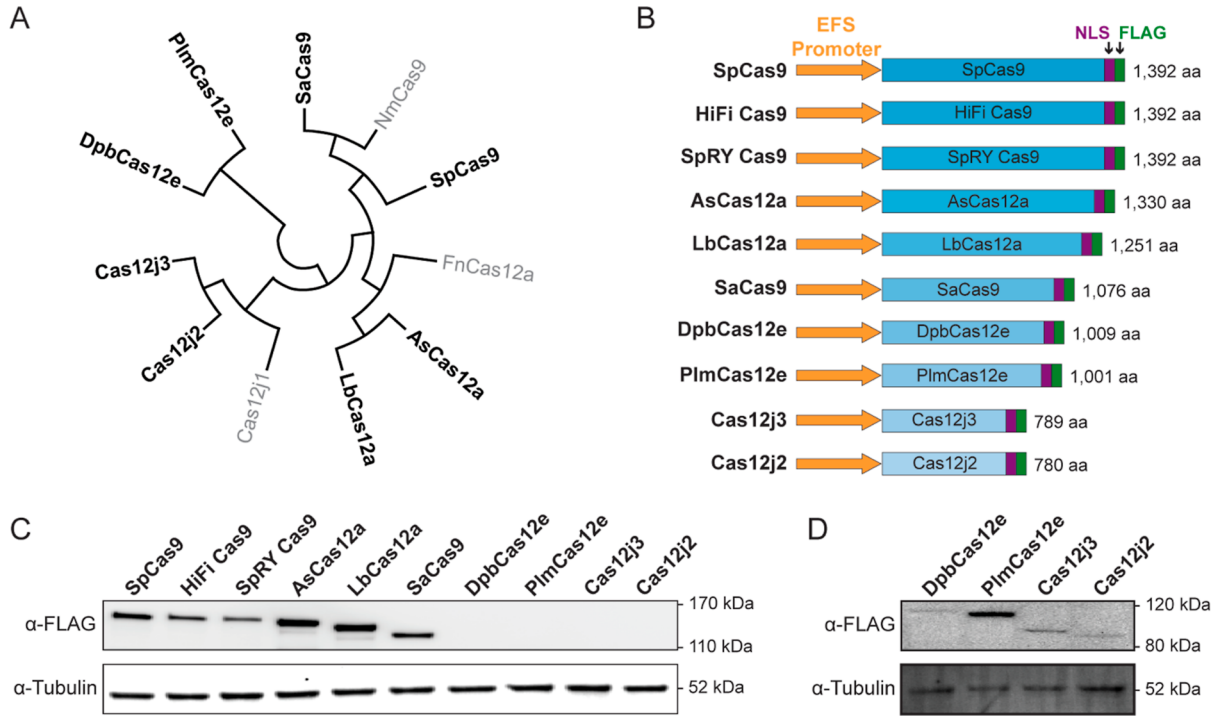

Figure 1. Cas enzymes display variable expression levels in human cells. (A) Phylogenetic topology among indicated Cas proteins. Cas proteins in gray are shown for comparative purposes and are not evaluated in this study. SpCas9; *Streptococcus pyogenes*Cas9, SaCas9; *Staphylococcus aureus*Cas9, NmCas9;*Neisseria meningitidis*Cas9, AsCas12a;*Acidaminococcus*sp. BV3L6 Cas12a, LbCas12a; *Lachnospiraceae bacterium* Cas12a, FnCas12a; *Francisella novicida* Cas12a, DpbCas12e; *Deltaproteobacteria* Cas12e, PlmCas12e; *Planctomycetes* Cas12e, Cas12j1; CasΦ1, Cas12j2; CasΦ2, and Cas12j3; CasΦ3. (B) Indicated Cas nucleases were expressed in isogenic vector backbones and are schematically depicted and ordered by respective size from the largest (top) to smallest (bottom). EFS; *EF1α* short promoter, NLS; nuclear localization sequence. (C,D) Indicated Cas nucleases were transiently co-transfected into HEK293T cells along with a corresponding non-targeting gRNA and 25 μg (panel C) or 50 μg (panel D) of total protein was probed via Western blot 72 h post-transfection.

nucleases, no corresponding CRISPRa or CRISPRi tools have been developed. Such tools could be particularly useful for endogenous gene activation or repression strategies in combination with smaller CRISPR/Cas systems (i.e., Cas12e and Cas12j).

Here, we selected 10 different CRISPR/Cas variants from both Type II and Type V families and developed a series of genome editing and CRISPRa/CRISPRi tools in isogenic expression vector backbones. We quantified the genome editing efficacy of each variant using different gRNA-targeted sites within an integrated eGFP testbed in the human HEK293T cell line. We also measured the genome editing efficacy of these different CRISPR nucleases at the endogenous *EMX1* locus in HEK293T, HeLa, and U2OS cells. Additionally, we evaluated the CRISPRi (using 10 different KRAB fusion proteins) and CRISPRa (using 10 different VPR fusion proteins) capabilities of each variant at endogenous human loci. Further, we designed integrated testbed frameworks to benchmark any of the selected CRISPRi/CRISPRa orthologues or variants at the same target site regardless of the respective PAM requirements. We find that across these human cell lines, Type II CRISPR/Cas systems generally outperform Type V systems in both genome editing and transcriptional activation, and that nearly all CRISPR/Cas systems permit transcriptional repression when fused to the KRAB domain. Collectively, our studies clarify the relative efficacies of diverse natural and engineered CRISPR/Cas systems in human cells and provide a useful set of new ready-to-use expression vectors and assay testbeds that can enable rapid and robust in situ comparisons among current and future genomic-targeted CRISPR/Cas variants.

RESULTS AND DISCUSSION

Cas Proteins from Different Families can Display Variable Expression Levels in Human Cells. The CRISPR/Cas-based genome editing toolbox has rapidly expanded in recent years, which in turn has established that Cas protein variants with different sizes (ranging in size from ∼400 to ∼1300 amino acids) and different PAM sequence specificities can function in human cells. Despite this exciting progress, systematic analyses to quantify the relative genome editing efficacies among these variants in human cells are lacking, particularly for newly described variants from the Cas12e and Cas12j families. To evaluate and compare the relative genome editing activities of these Cas protein variants, we selected 10 Cas enzymes (Figure 1A) including natural and engineered variants from the Cas9 and Cas12a families (SpCas9, HiFi Cas9, SpRY Cas9, SaCas9, AsCas12a, and LbCas12a),[3,6,25,26,30] and variants from the more recently described Cas12e and Cas12j families (DpbCas12e, PlmCas12e, Cas12j2, and Cas12j3).[7,9] We cloned each of these Cas proteins into an isogenic expression vector backbone such that each Cas protein harbored a nuclear localization sequence (NLS), a FLAG epitope tag, and was transcribed by the core EF1α shortened (EFS) promoter (Figure 1B).

We transiently co-transfected each Cas variant-encoding vector along with a second vector expressing a corresponding, species-matched gRNA scaffold and a non-targeting control

https://doi.org/10.1021/acssynbio.2c00156
ACS Synth. Biol. 2022, 11, 3239−3250

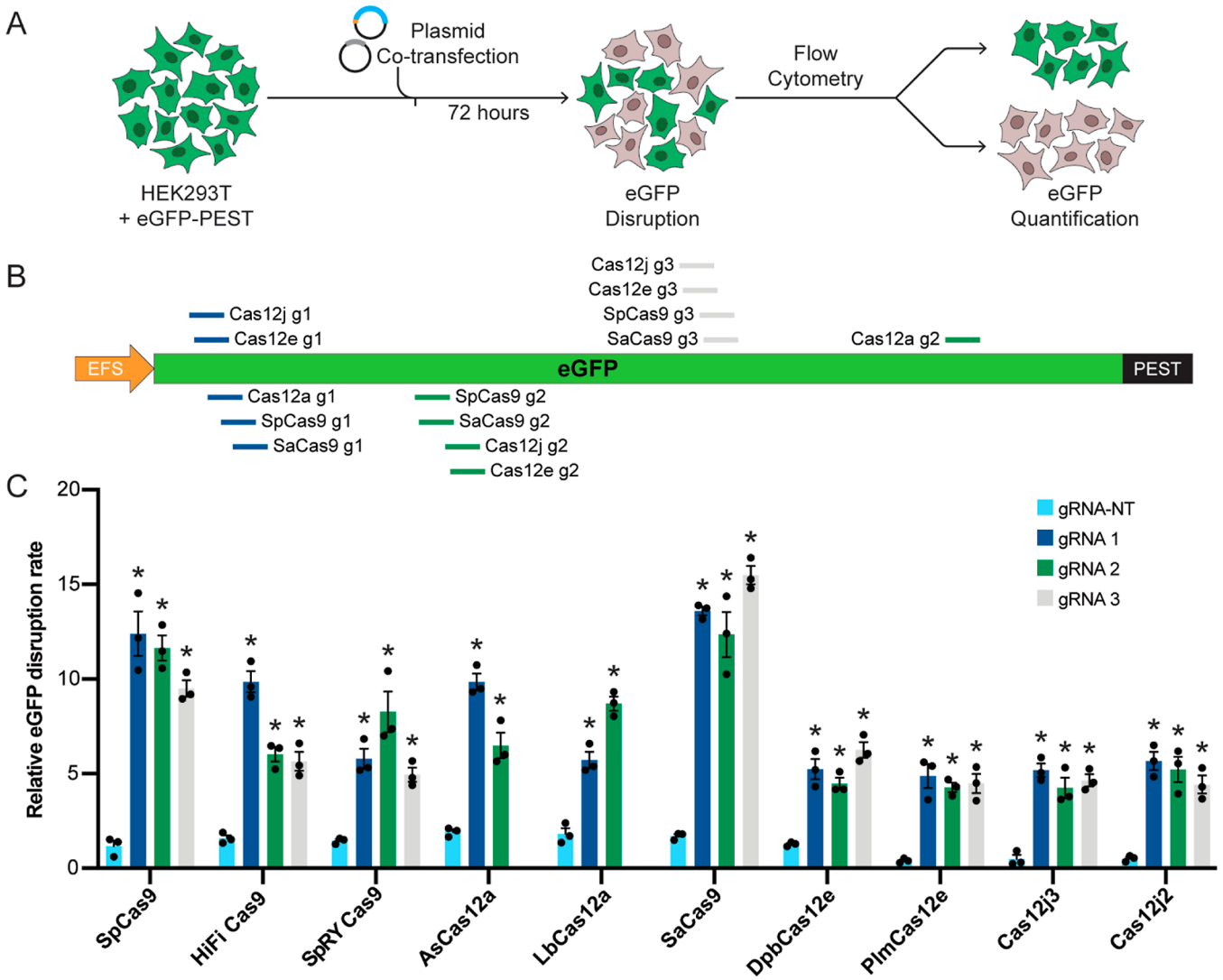

Figure 2. Genome editing efficacy differs between Cas variants in human cells. (A) Experimental workflow used to quantify genome editing efficacy among different Cas protein variants. (B) Guide RNAs (gRNAs) targeting eGFP are indicated for respective Cas proteins. gRNAs (2 to 3 depending on Cas protein variant) are color coded based upon their targeted location (5′−3′) within eGFP. (C) Relative eGFP disruption rates were calculated by counting the percentage of cells that lost eGFP 72 h after transfection with indicated Cas orthologues or variants and respective gRNAs. Data presented as mean ± s.e.m; *P < 0.05 (Student's t-test); n = 3 independent experiments.

protospacer (Table S1) into HEK293T cells to first evaluate relative expression levels among Cas protein variants in human cells using Western blotting. Interestingly, despite controlled transfection conditions, isogenic vector designs, and reported optimizations for all tested Cas variants in human cells,[4−7,9,25,26,30] differing expression levels were observed 72 h post-transient co-transfection in HEK293T cells (Figures 1C and S2). For instance, although Cas12a and Cas9 family members were generally well expressed, Cas12e and Cas12j family members were relatively poorly expressed. In fact, Cas12e and Cas12j variants were only detectable via Western blotting with higher total protein loading amounts (∼50 μg) and longer exposure times (∼600 s; Figure 1D). Flow cytometry to detect the FLAG epitope on the C-terminus of each nuclease active Cas variant in transfected HEK293T cells recapitulated our Western blotting results (Figure S2). Interestingly, the differences between the expression levels of these Cas variants in HEK293T cells were not due to differences in the amounts of respective plasmids transfected into cells (Figure S3).

Different Cas Nucleases Exhibit Variable Genome Editing Efficacies in Human Cells. We next tested the relative efficacies among these 10 selected Cas variants for targeted insertions and deletions (indels) in HEK293T cells using an eGFP disruption assay (Figure 2A). Multiple gRNAs targeting eGFP were designed for each Cas variant to maximize comparative analysis. gRNAs were also selected to target as closely as possible to one another (given PAM sequence restrictions). For Cas12a variants, only two different gRNAs targeting eGFP were available to test disruption efficacy, whereas for all other variants we tested disruption efficacy using three different gRNAs targeting eGFP (Figures 2B and S4). eGFP was integrated into a master HEK293T cell line at a multiplicity of infection (MOI) of ∼10.0 and then eGFP positive cells were sorted, collected, and tested as bulk cell populations. Bulk cells were used to ensure that the eGFP expression was equivalently distributed across all experimental conditions. Similarly, an MOI of ∼10.0 was used to normalize chromatin landscapes at integration sites across all experiments. We also introduced a PEST domain on the C-terminus

https://doi.org/10.1021/acssynbio.2c00156
ACS Synth. Biol. 2022, 11, 3239−3250

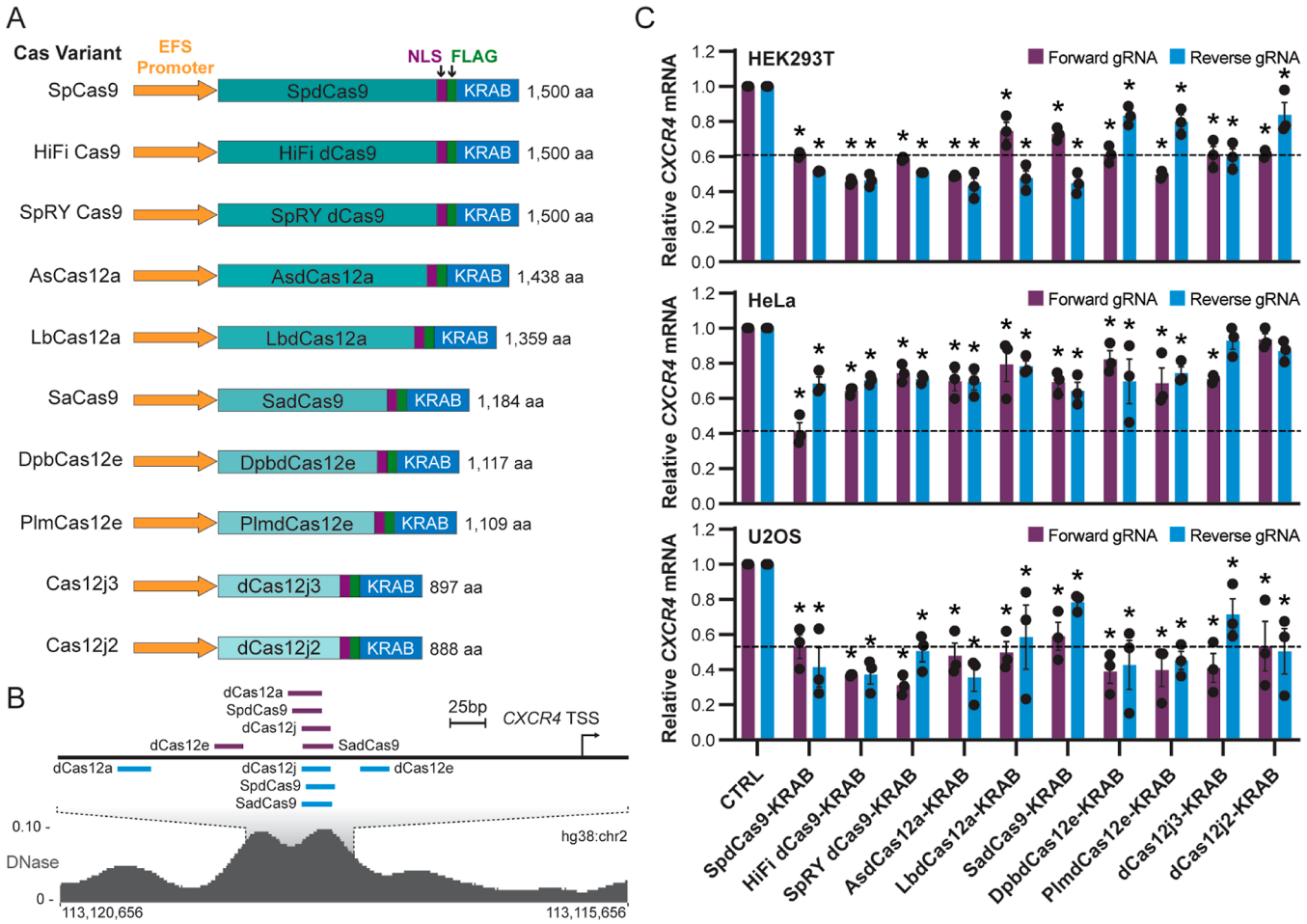

Figure 3. Diverse Cas proteins are compatible with KRAB-mediated CRISPRi at the human *CXCR4* locus. (A) Schematics of 10 indicated dCas-KRAB fusions encoded by isogenic vector backbones. EFS; *EF1α* short promoter, and NLS; nuclear localization sequence. (B) gRNAs targeting the *CXCR4* promoter associated with indicated dCas variants are shown. DNase accessibility in HEK293T cells (GSM1635901) is also shown. gRNAs on the forward and reverse genomic strands are shown in purple and light blue, respectively. TSS; transcription start site. (C) Relative *CXCR4* mRNA expression (compared to cells transfected with empty vector; mock transfected, "CTRL") 72 h post-transfection of indicated dCas-KRAB fusion protein variants and corresponding *CXCR4* promoter-targeting gRNAs in HEK293T (top), HeLa (middle), and U2OS (bottom) cells. Dashed line denotes *CXCR4* expression when targeted by the SpdCas9-KRAB fusion protein and the indicated forward gRNA. Data presented as mean ± s.e.m; $*P < 0.05$ (Student's *t*-test); $n = 3$ independent experiments.

of eGFP to reduce eGFP background/half-life, similar to previously described assay designs.[35,36]

Despite variable expression levels among tested Cas variants, all Cas enzymes were able to significantly disrupt the eGFP expression at all gRNA-targeted sites relative to non-targeting gRNA control-treated HEK293T cells (Figure 2C). Consistent with previous reports,[37] SaCas9 displayed comparable, yet measurably higher genome editing efficacy compared to SpCas9. Regardless, SpCas9 and SaCas9 both displayed slightly better nuclease activities than Cas12a variants (AsCas12a and LbCas12a). Further, Cas12j family enzymes (Cas12j2 and Cas12j3) exhibited the lowest nuclease activities in this controlled testbed system (Figure 2C). Finally, as has been observed previously at some loci,[25,26] the engineered HiFiCas9 and SpRYCas9 variants (derived from WT SpCas9), displayed slightly lower indel rates than WT SpCas9.

To extend our analysis beyond this eGFP testbed system, we targeted each Cas nuclease to the endogenous *EMX1* locus in HEK293T, HeLa, and U2OS cells (Figure S5A). Tracking of indels by decomposition (TIDE) analysis[38] at *EMX1* largely replicated the trends observed at the testbed locus (Figure S5B). These trends were most consistent among HEK293T and HeLa cells, and to a lesser extent in U2OS cells. Regardless, these data indicate that although there may be a hierarchy of nuclease efficacy among Cas variants (i.e., Cas9 ≥ Cas12 > Cas12j) in human cells, each enzyme is capable of effective genome editing within human cells.

Diverse Cas Proteins Are Compatible with KRAB-Mediated CRISPRi in Human Cells. The intrinsic nuclease activity of Cas proteins can be deactivated through mutagenesis of catalytic amino acid residues. These nuclease-deactivated Cas (dCas) proteins have revolutionized the ability to alter the endogenous human epigenome and/or activate or repress human genes using CRISPRa and CRISPRi approaches, respectively.[12−19,39−45] Although targeting a dCas protein to a human promoter can, in some cases, result in reduced downstream gene expression, this inhibitory effect is more consistent, and often amplified, by fusing a Krüppel-associated box (KRAB) domain to the C-terminus of the dCas9 protein.[12,46] Therefore, we fused a KRAB domain to the C-terminus of 10 nuclease-deactivated Cas9, Cas12a, Cas12e, or Cas12j proteins in isogenic vector backbones (Figure 3A) to

https://doi.org/10.1021/acssynbio.2c00156
ACS Synth. Biol. 2022, 11, 3239−3250

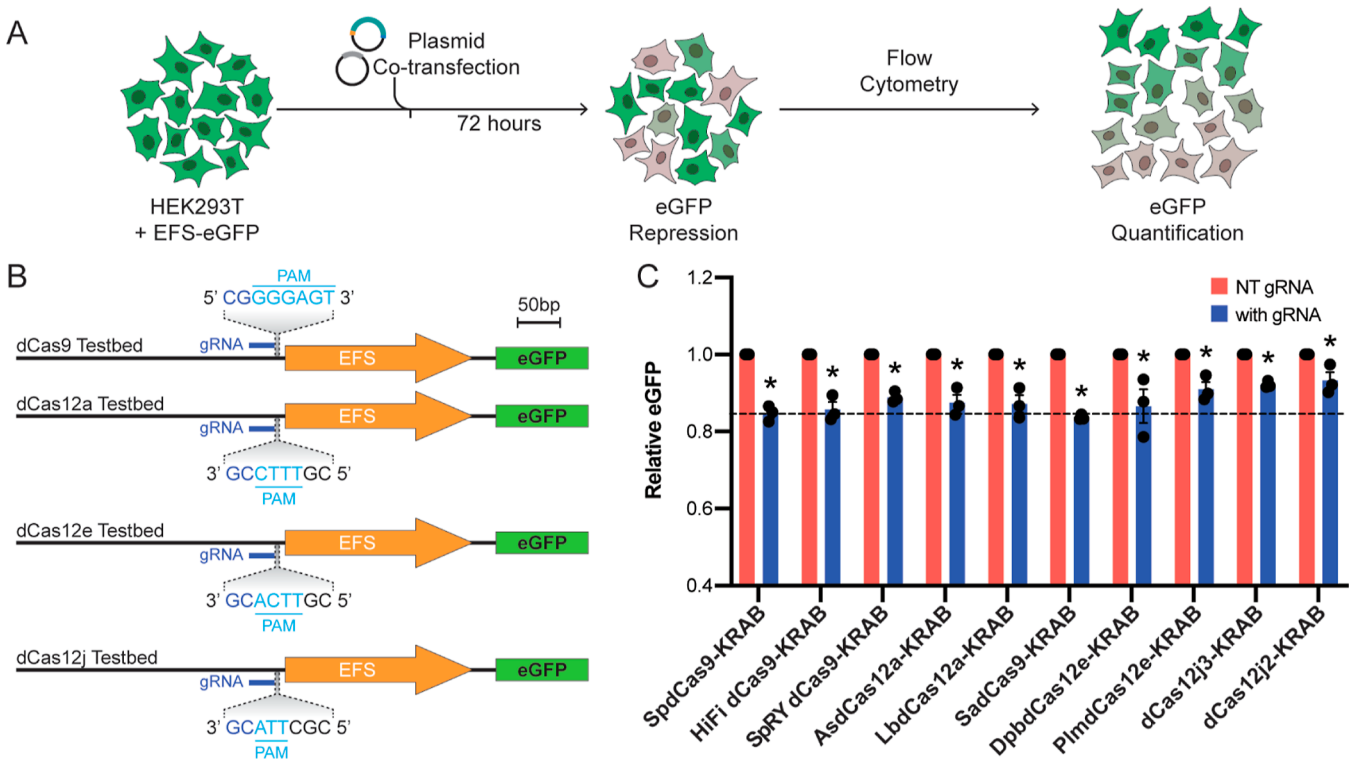

Figure 4. Diverse Cas proteins are compatible with KRAB-mediated CRISPRi at a synthetic testbed locus in human cells. (A) Experimental workflow used to quantify genome CRISPR interference (CRISPRi) efficacy among different Cas protein variants fused to the KRAB repressor domain. (B) CRISPRi testbed systems are schematically depicted along with respective gRNAs and PAM sequences/orientations. EFS; *EF1α* short promoter. (C) Relative eGFP (fold change vs a non-targeting gRNA; "NT gRNA") measured by flow cytometry 72 h post-transfection of indicated dCas-KRAB fusion protein expression vectors and corresponding gRNAs, dotted line denotes the repression level of SpdCas9-KRAB. Data presented as mean ± s.e.m; *$P < 0.05$ (Student's *t*-test); $n = 3$ independent experiments. Cas12e and Casd12j systems can display poor CRISPRa potencies in human cells.

quantify the relative abilities of variants from these families to repress gene expression in human cells. Interestingly, we observed that the fusion of a KRAB domain to the C-terminus of Cas proteins resulted in slight changes to their relative expression in HEK293T cells (Figure S6). Nevertheless, when targeted to the endogenous human *CXCR4* promoter in HEK293T or U2OS cells (Figure 3B), all dCas-KRAB variants displayed significant ($P < 0.05$) repression of *CXCR4* transcription relative to mock transfected control cells (Figure 3C, top and bottom). In HeLa cells, all dCas-KRAB variants were also capable of significant ($P < 0.05$) repression of *CXCR4* transcription relative to mock transfected control cells with the exception of dCas12j2-KRAB (Figure 3C, middle). This trend was largely consistent across gRNAs targeting either forward or reverse genomic strands, although effects related to gRNA orientation and/or relative distance from the *CXCR4* TSS were evident for some Cas variants.

Although we designed *CXCR4*-targeting gRNAs for each respective dCas-KRAB variant to be as close as possible to one another, an exact target overlap within the native human genome is currently impossible due to differing PAM sequence requirements. Therefore, to more precisely compare the repressive capacities of each dCas-KRAB variant, we created four equivalent CRISPRi lentiviral testbeds that varied only in terms of which PAM sequence (5′-GGGAGT-3′ for Cas9 proteins, 5′-TTTC-3′ for Cas12a proteins, 5′-TTCA-3′ for Cas12e, and 5′-TTA-3′ for Cas12j proteins, respectively) was placed upstream of an EFS promoter constitutively driving eGFP (Figures 4B and S7A). All PAMs were next to a synthetically introduced protospacer without predicted genomic off-targets,[47,48] which enabled us to target each CRISPRi tool to the same exact sequence/spacing upstream of the integrated EFS promoter. Each respective eGFP expressing testbed was integrated into HEK293T cells at an MOI of ∼10.0 to generate 4 master HEK293T cell lines (Figure 4A) and further, eGFP positive cells were sorted, collected, and tested as bulk cell populations. As above, these steps were taken to equilibrate distribution of eGFP expression and normalized chromatin landscapes at integration sites across all experiments. Similar to our results at the endogenous *CXCR4* locus, all tested dCas-KRAB variants significantly ($P < 0.05$) repressed eGFP expression when targeted 16bp upstream of the EFS promoter in testbed systems in HEK293T cells (Figures 4C and S8). These data demonstrate that all tested nuclease-inactivated CRISPR/Cas systems from Type II and Type V families are capable of human gene repression when fused to the KRAB domain and that our testbed CRISPRi platform enables rapid, simple, and robust quantification of the relative efficacy of diverse CRISPRi tools or even repressive dCas-based epigenome editing technologies[49,50] in future iterations.

dCas proteins have also been used to activate endogenous genes in so-called CRISPRa settings wherein the dCas protein is used as a scaffold to recruit transcriptional activation domains to regulatory elements such as promoters or enhancers.[12−19,29,32,39−45] One such CRISPRa system leverages a tripartite transcriptional activation domain called VPR (VP64-p65-Rta) fused the C-terminus of a dCas protein.[14] To

https://doi.org/10.1021/acssynbio.2c00156
ACS Synth. Biol. 2022, 11, 3239−3250

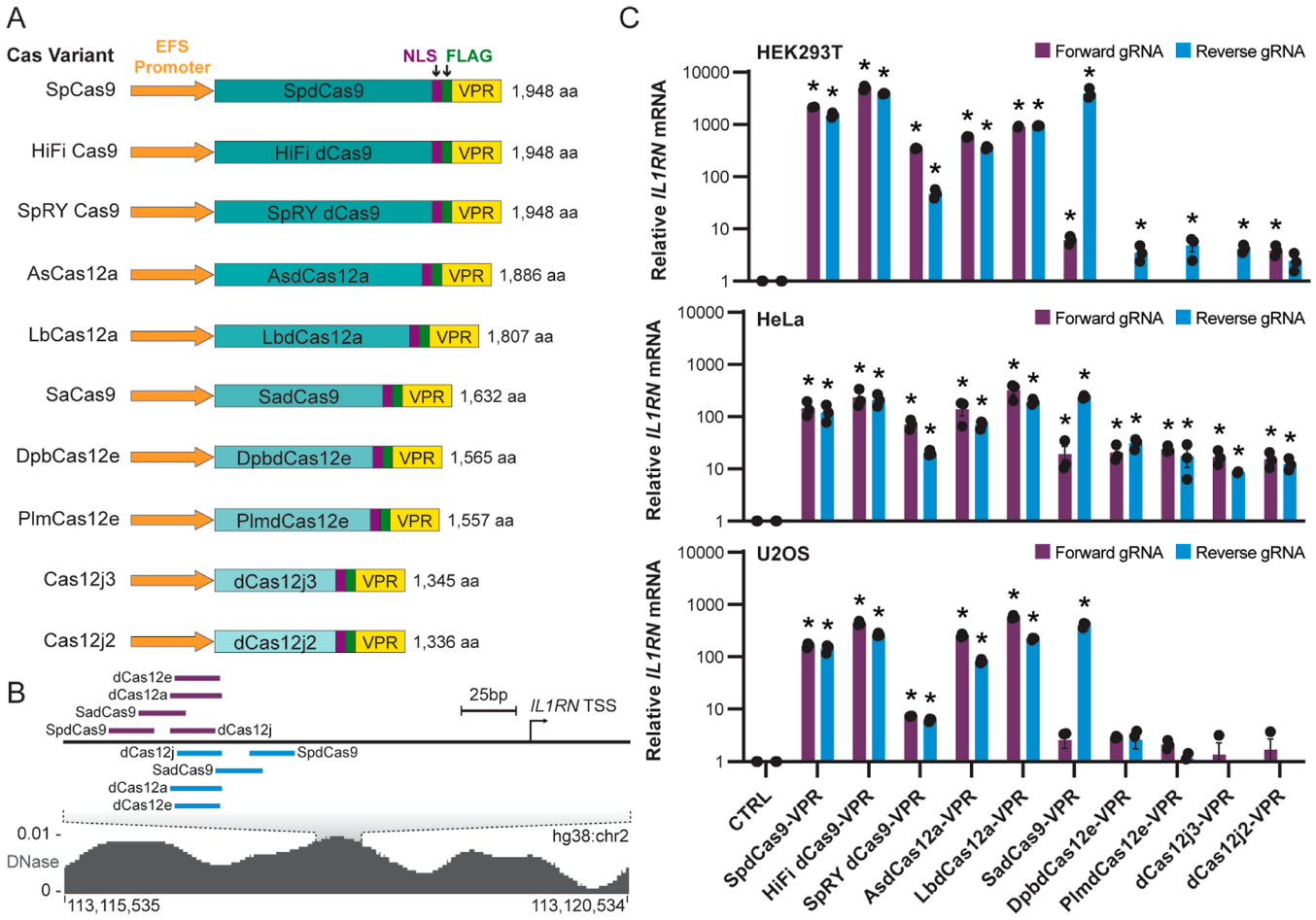

Figure 5. Relative CRISPRa potencies vary among Cas proteins at the *IL1RN* promoter. (A) Schematics of 10 indicated dCas-VPR fusions encoded by isogenic vector backbones. EFS; *EF1α* short promoter, NLS; nuclear localization sequence. (B) Schematic of the human *IL1RN* locus including gRNAs on the forward (purple) and reverse (light blue) genomic strands, respectively, used to target indicated dCas-VPR fusions. DNase accessibility is also shown (GSM1635901). (C) Relative *IL1RN* expression (compared to cells transfected with empty vector; mock transfected, "CTRL") 72 h post-transfection of the indicated dCas-VPR fusion proteins and corresponding *IL1RN* promoter-targeting gRNAs in HEK293T (top), HeLa (middle), and U2OS (bottom) cells. Data presented as mean ± s.e.m; $^*P < 0.05$ (Student's t-test); $n = 3$ independent experiments.

measure the relative abilities of dCas variants to activate transcription in human cells, we fused the VPR domain to the C-termini of the selected dCas9, dCas12a, dCas12e, or dCas12j proteins in the isogenic vector backbones (Figure 5A). As observed with the KRAB domain, fusion of the VPR domain to the C-terminus of different dCas proteins resulted in reduced protein expression in HEK293T cells (Figure S9). Despite this effect, when targeted to the human *IL1RN* promoter (Figure 5B) in HEK293T and HeLa cells, all dCas-VPR variants displayed the ability to activate endogenous *IL1RN* expression, albeit relatively inconsistently among variants (Figure 5C, top and middle). In U2OS cells, although Type II dCas-VPR variants were capable of significant ($P < 0.05$) activation of *IL1RN* transcription relative to mock transfected control cells, Type V dCas-VPR fusions were markedly less effective (Figure 5C, bottom). Together this indicates that overall dCas9/dCas12a-VPR fusions were more effective at activating *IL1RN* gene expression than dCas12e/dCas12j-VPR fusions in these three human cell lines.

Again, because targeting each respective dCas-VPR variant to the same exact sites within the native human genome is currently impossible due to differing PAM sequence requirements, we created four equivalent CRISPRa lentiviral testbeds (Figure S7B) to more systematically compare the trans-activation capacities of selected dCas-VPR variants (Figure 6A). Similar to our CRISPRi testbeds, each CRISPRa lentiviral testbed varied only in terms of which PAM sequence (5′-GGGAGT-3′ for Cas9 proteins, 5′-TTTC-3′ for Cas12a proteins, 5′-TTCA-3′ for Cas12e, and 5′-TTA-3′ for Cas12j proteins, respectively) was placed upstream of a target promoter that could drive the eGFP expression when stimulated (Figure 6B). However, for these CRISPRa testbed experiments, the miniCMV promoter was selected to drive eGFP in response to dCas-VPR variants because it has been found to display low basal expression and to be highly responsive to the VPR domain in human cells.[14] All PAMs were designed next to a synthetically introduced protospacer without predicted genomic off-targets,[47,48] which enabled us to target each CRISPRa tool to the same exact sequence/spacing upstream of the integrated miniCMV promoter.

As shown above, each respective miniCMV-eGFP testbed was integrated into HEK293T cells at an MOI of ∼10.0 to generate 4 master HEK293T cell lines (Figure 6A). Transduced cells were tested as bulk cell populations to ensure an equivalent distribution of eGFP expression and normalized chromatin landscapes at integration sites across all experiments. All dCas-VPR variants significantly ($P < 0.05$) upregulated eGFP expression when targeted 16bp upstream of

https://doi.org/10.1021/acssynbio.2c00156
ACS Synth. Biol. 2022, 11, 3239−3250

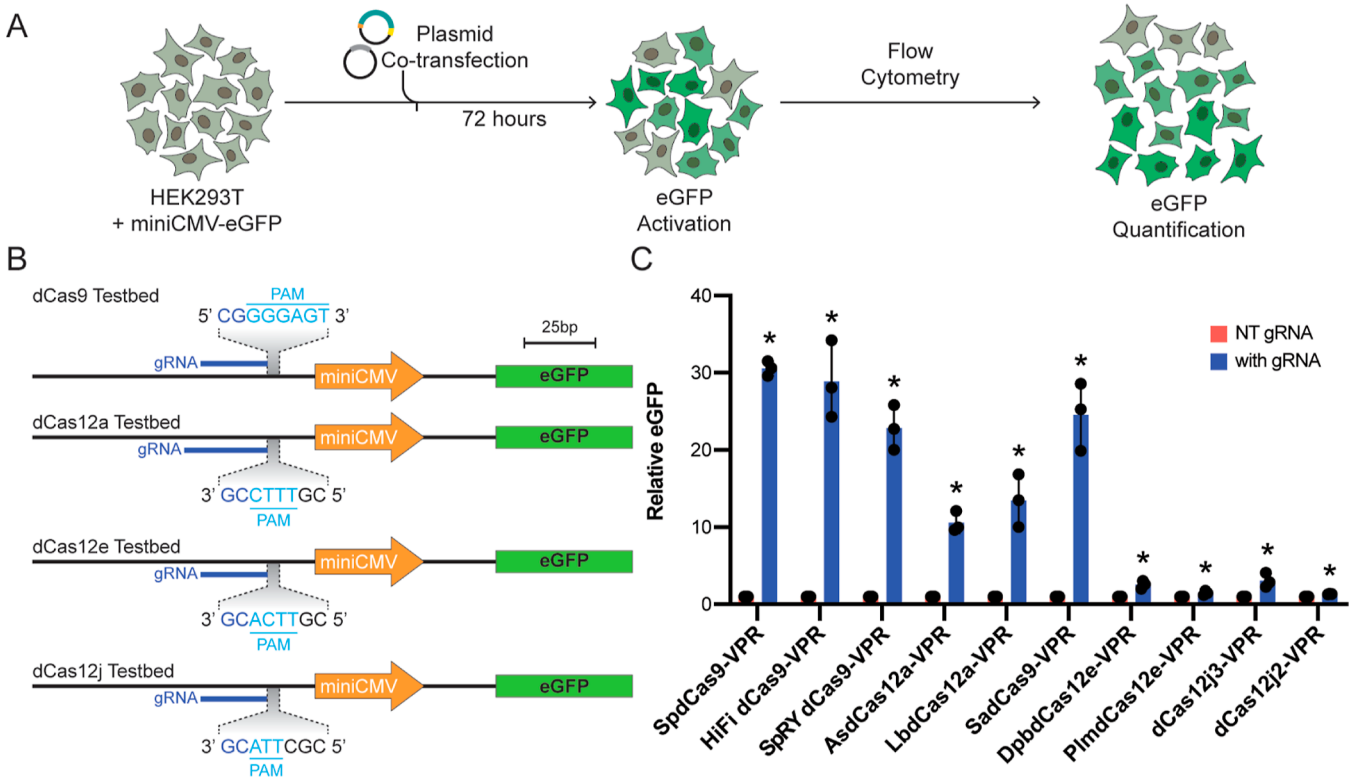

Figure 6. Cas proteins exhibit varying CRISPRa potencies at a synthetic testbed locus in human cells. (A) Experimental workflow used to quantify genome CRISPR activation (CRISPRa) efficacy among different Cas protein variants fused to the VPR activation domain. (B) CRISPRa testbed systems are schematically depicted along with respective gRNAs and PAM sequences/orientations. miniCMV; mini Cytomegalovirus immediate early promoter. (C) Relative eGFP (fold change vs a non-targeting gRNA; "NT gRNA") measured by flow cytometry 72 h post-transfection of indicated dCas-VPR fusion protein expression vectors and corresponding gRNAs. Data presented as mean ± s.e.m; *$P < 0.05$ (Student's *t*-test); $n = 3$ independent experiments.

the miniCMV promoter (Figure 6C). However, overall Cas9 family enzymes performed the best in CRISPRa testbed assays (up to ~30-fold activation) followed by Cas12a family variants (up to ~15 fold activation). Although the CRISPRa tools based on Cas12e and Cas12j family variants only slightly activated eGFP expression (up to ~3 fold), this was nonetheless significantly ($P < 0.05$) above non-targeting gRNA control-treated HEK293T cells. Collectively, these results suggest that all nuclease-inactivated CRISPR systems are capable of human gene activation when fused to the VPR domain but that Cas12e and Cas12j family variants are less effective than Cas9 and Cas12a systems. Finally, these data support the use of our testbed CRISPRa platform as a robust and straightforward framework to rapidly evaluate and benchmark CRISPRa technologies.

The recent expansion of CRISPR/Cas-based tools available for use in human cells has transformed the ability to reshape the human genome, transcriptome, and epigenome. Nevertheless, a lack of clarity exists surrounding the relative endogenous efficacies of these powerful technologies. Consequently, the selection of an optimal CRISPR/Cas system for a particular application has been unnecessarily challenging, and this challenge in turn has limited the adoption of otherwise extremely useful synthetic biology technologies. Here, we designed a series of robust integrated testbeds to systematically compare the genome editing, CRISPRi, and CRISPRa capabilities of both the most commonly used, and newly developed, CRISPR/Cas systems to address this lack of clarity. Our results demonstrate that although all Cas protein variants are generally capable of genome editing and transcriptional control, some variants outperform others in human HEK293T cells. We also built 20 different Cas fusion proteins in isogenic expression vector backbones that can be used for CRISPRi and CRISPRa applications across different PAM targeting and specificity landscapes. Our findings here highlight the utility of our optimized testbed platforms to limit the variables that can confound effective comparisons among current, and future CRISPR/Cas variants in human, or other cell types.

Our results here using these testbeds reveal an apparent hierarchy among Cas variants in terms of genome editing and CRISPRa efficacies in human cells. Specifically, Cas9 variants (i.e., WT SpCas9, SpCas9 derivatives, and WT SaCas9) generally perform comparably to one another and perform as well as, or better than, Cas12a variants. However, Cas9 and Cas12a systems both outperform Cas12e or Cas12j variants in our experimental systems (Figures 2, 5, and 6). Interestingly, although Cas12e and Cas12j variants showed moderate genome editing activity (Figures 2C and S5B), each variant displayed only weak gene activation capabilities at both endogenous and synthetic loci when fused to the VPR effector domain (Figures 5C and 6C). This result is consistent with a recent study focusing on another small Type V CRISPR/Cas family member; Cas12f (also called Cas14), which found that dCas12f-VPR could only activate human genes after substantial engineering of the corresponding gRNA and dCas12f protein (the CasMini system).[51] These results suggest that there is a high likelihood that protein and/or gRNA engineering efforts could also improve the genome editing and/or CRISPRa

https://doi.org/10.1021/acssynbio.2c00156
ACS Synth. Biol. 2022, 11, 3239−3250

activities of Cas12e and Cas12j variants in human cells, although by design our goal here was to benchmark selected Cas variants with minimal manipulation relative to published compositions.

In contrast to the variation observed in genome editing and CRISPRa activities, all tested CRISPR/Cas systems displayed relatively consistent CRISPRi potencies at both endogenous and testbed targets when fused to the KRAB domain (Figures 3C and 4C). This difference between CRISPRi (using the KRAB domain) and CRISPRa (using the VPR domain) effects could be due to the relatively small size of the fused KRAB domain (~65aa) compared to the VPR domain (~531aa). Alternatively (and not mutually exclusive), these variations could be due to intrinsic mechanistic differences between endogenous gene activation vs gene repression. Interestingly, our data demonstrate that although the fusion of transcriptional effectors to Cas proteins can reduce their relative expression, and the magnitude of this reduction can be more dramatic for VPR fusions than for fusions containing the KRAB effector (Figures S6 and S9), the tools nonetheless generally retain respective functionality. Whether engineering efforts that result in increased expression would translate into increased CRISPRi/a, or even CRISPR nuclease, potencies, remains to be determined.

Notably, the inconsistencies observed among Cas variants could also be driven by differences in relative gRNA/crRNA binding affinities among different Cas proteins. For instance, the crRNA binding affinity of Cas12a has been observed to be lower than that of Cas9,[52−55] which could partly explain why Cas12a (or dCas12a-VPR fusions) might not edit (or activate) genes as robustly as Cas9 family enzymes (or dCas9-VPR fusions). Additionally, gRNA/crRNA activity could be gRNA/crRNA sequence dependent. Regardless, our results show that Cas12a is an effective endonuclease in human cells, and given the smaller size, potential for multiplexing, reports of reduced off-targeting, and findings that the Cas12a system is amenable to engineered enhancement,[53,55−63] it, therefore, is a very promising emergent technology. Similarly, the KRAB/VPR fusions based on SadCas9 generally showed a comparable efficacy in CRISPRi/a relative to SpdCas9-based tools (Figures 3C, 4C, 5C, and 6C). Moreover, SaCas9 performed slightly better than SpCas9 in our disruption assays (Figures 2C and S5B). Therefore, SaCas9 derivatives are excellent alternatives to SpCas9 proteins, especially in applications where the payload size is restricted, such as AAV delivery.

Altogether, our studies demonstrate that CRISPR/Cas systems from diverse families are useful for applications in genome editing and transcription modulation within human cells. However, using our controlled isogenic expression cassettes, we found that different Cas variants can have inconsistent expression levels, at least in HEK293T cells. Furthermore, we find that the genome editing and CRISPRa efficacies are not equivalent among different CRISPR systems at both endogenous sites and at carefully designed testbed systems wherein experimental variables, aside from which Cas variant is tested, were minimized. In fact, our data using these tightly controlled experimental settings indicate that there is a hierarchy for relative genome editing and CRISPRa activities among the 10 different Cas variants that we tested here in which Cas9 performs better than or as good as Cas12a and both Cas9 and Cas12a outperform Cas12e/Cas12j. Given the biological nuances distinguishing different Cas variants, there is simply no system with which to benchmark them perfectly. However, our testbed frameworks described here provide a powerful and effective method to evaluate the relative activities of current, or future CRISPR/Cas systems that target genomic DNA in practically any mammalian cell that can be transduced or transfected. Therefore, as more CRISPR/Cas systems continue to be discovered and optimized for use in mammalian/human cells, the technologies that we have described here can be used to rapidly and quantitatively compare their endogenous efficacies. These testbeds could also be useful in screening for improved functions of engineered Cas proteins in endogenous contexts in a high throughput. Collectively, our studies and these new quantitative capabilities can help foster the adoption, implementation, and improvement of the rapidly expanding CRISPR/Cas-based toolbox and thereby augment their utility in providing innovative opportunities across basic and applied biomedical research.

METHODS

Phylogenetic Analysis. 18 Cas protein sequences were retrieved from Genbank and/or previous reports then analyzed using the multiple sequence alignment program MUSCLE.[64] Phylogenetic tree topology diagrams were generated using the Maximum Likelihood method via the MEGA X software package.[65] Sequence identities for SpCas9, SaCas9, NmCas9, AsCas12a, LbCas12a, FnCas12a, DpbCas12e, PlmCas12e, Cas12j2 (CasΦ2), and Cas12j3 (CasΦ3) were generated from WP_032462936.1, AXB99496.1, MBH2503069.1, WP_021736722.1, QRU95066.1, WP_216372291.1, OGP07438.1, OHB99618.1, PDB: 7LYS_A, and PDB: 7ODF_A, respectively. Sequence identity for Cas12j1 (CasΦ1) was derived from a previous report.[9]

Plasmid Constructs. All plasmids encoding Cas protein variants and all testbed vectors constructed in this work are available through Addgene. SpCas9, HiFi Cas9, SpRY, AsCas12a, LbCas12a, DpCas12e, PxCas12e, Cas12j2, and Cas12j3 nucleases were polymerase chain reaction (PCR)-amplified from lentiCRISPR v2 (Addgene, 52961), pX165-HiFi Cas9 (Addgene, 140563), pCMV-T7-SpRY-P2A-EGFP (RTW4830; Addgene, 139989), pY026 (Addgene, 84741), pY027 (Addgene, 84742), pBLO 62.4 (Addgene, 123123), pBLO 62.5 (Addgene, 123124), pPP441 (Addgene, 158801), and pPP444 (Addgene, 158802), respectively. SaCas9 sequence was based on pX600-AAV-CMV:NLS-SaCas9-NLS-3xHA-bGHpA (Addgene, 61592). The nuclease inactivated HiFidCas9 (D10A/H840A mutations), and SpRYdCas9 (D10A/H840A mutations), AsdCas12a (D908A mutation), LbdCas12a (D832A mutation), SadCas9 (D10A and N580A mutations), DpdCas12e (D672A/E769A/D935A mutations), PxdCas12e (D659A/E756A/D922A mutations), dCas12j3 (D413A mutations), and dCas12j2 (D394A mutation) were PCR-amplified using corresponding primer sets designed to engender-specified nuclease-inactivating mutations. Nuclease active and inactivated Cas plasmids were constructed by cloning PCR-amplified fragments into the AfeI and BamHI digested dCas9-dMSK1-P2A-Puro plasmid backbone described previously (Addgene, 165602) via a NEBuilder HiFi DNA Assembly (NEB, E2621). The VPR and KRAB effector domains were amplified from SP-dCas9-VPR (Addgene, 63798) and hUbC-dCas9-KRAB-T2A-Puro (Addgene, 71236), respectively, and cloned into each corresponding BamHI digested dCas plasmid backbone via a NEBuilder HiFi DNA Assembly. The parental CRISPRa testbed plasmids was created by assembling the EcoRI- and MluI-digested dCas9-

https://doi.org/10.1021/acssynbio.2c00156
ACS Synth. Biol. 2022, 11, 3239−3250

dMSK1 (Addgene, 63799) together with a PCR-amplified hPGK promoter (Addgene, 63799), a PCR-amplified Blasticidin resistance gene (Addgene, 63799), a PCR-amplified eGFP gene, and a commercially synthesized fragment (gBlock, IDT) harboring NheI and XhoI cut sites upstream of miniCMV. The parental CRISPRi testbed plasmid was created by digesting with the parental CRISPRa testbed plasmid with EcoRI and MluI and then cloning in an EFS promoter (Addgene, 63798) via NEBuilder HiFi DNA Assembly. Each subsequent CRISPRa or CRISPRi testbed plasmid was made by digesting the corresponding parental plasmid with NheI and XhoI and ligating two annealed oligos encoding specified PAM and protospacer sequences. SpCas9-associated gRNAs were cloned into pSPgRNA (Addgene 47108). SaCas9-associated gRNAs were cloned into a pZDonor plasmid containing an SaCas9-gRNA scaffold cassette downstream of hU6 promoter. The gRNA scaffold cassettes for AsCas12a, LbCas12a, Cas12e, Cas12j2, and Cas12j3 were PCR-amplified from pY026 (Addgene, 84741), pY027 (Addgene, 84742), pPP441 (Addgene, 158801), and pPP444 (Addgene, 158802), respectively, and then cloned into NdeI and SacII digested pSPgRNA (Addgene 47108). The gRNAs for each Cas were cloned into the compatible gRNA backbones. All gRNA protospacer sequences are shown in Table S1. Amino acid sequences for Cas constructs are shown in Supporting Notes 1−3.

Cell Lines and Transfections. HEK293T (ATCC and CRL-11268) and HeLa cells (ATCC and CCL-2) were cultured in Dulbecco's modified Eagle's medium (Gibco, 31-053-028) supplemented with 10% FBS (Sigma, F2442) and 1% penicillin/streptomycin at 37 °C and 5% CO2. U2OS cells (ATCC, HTB-96) were cultured in a McCoy's 5A (modified) medium (Gibco, 16-600-082) supplemented with 10% FBS (Sigma, F2442) and 1% penicillin/streptomycin at 37 °C and 5% CO2. Transient transfections were performed in 24-well plates using 375 ng of Cas or dCas (nuclease inactivated) expressing vector and 125 ng of corresponding gRNA vectors. Plasmids were transfected using Lipofectamine 3000 (ThermoFisher, L3000015) following manufacturer's instructions.

Lentiviral Production. One day before transfection, HEK293T cells were seeded at ∼40% confluency in a 10 cm plate. The next day cells were transfected at ∼80−90% confluency. For each transfection, 10 μg of plasmid containing the vector of interest, 10 μg of pMD2.G (Addgene, 12259), and 15 μg of psPAX2 (Addgene, 12260) were transfected using calcium phosphate. Five hours post-transfection the media was changed. The supernatant was harvested 24 and 48 h post-transfection and filtered with a 0.45 μm PVDF filter (Millipore, SLGVM33RS), and then the virus was concentrated using a Lenti-X Concentrator (Takara, 631232), aliquoted, and stored at −80 °C until use. Lentiviral titers were measured using a Lenti-X qRT-PCR Titration Kit (Takara, 631232).

Western Blotting. SDS-page gels were loaded with 25 or 50 μg of total protein and transferred onto a PVDF membrane (Bio-Rad, 1704274) using semi-dry electroblotting (Bio-Rad, 1704150) according to manufacturer's instructions. Mouse primary α-FLAG antibody (Sigma-Aldrich, F1804) was diluted at 1:1000 in Tris-Buffered Saline with 1% Casein (Bio-Rad, 1610782) and secondary α-mouse HRP-conjugated antibody (Cell Signaling, 7076) was used at a 1:3000 dilution in Tris-Buffered Saline with 1% Casein (Bio-Rad, 1610782). Membranes were incubated in an enhanced chemiluminescence substrate (ECL, Bio-Rad, 1705062). Tubulin was detected with a human α-Tubulin Rhodamine-conjugated antibody (Bio-Rad, 12004165) at a 1:3000 dilution in Tris Buffered Saline With 1% Casein (Bio-Rad, 1610782).

Intracellular Staining and Flow Cytometry. Transfected cells were trypsinized and then washed with phosphate-buffered saline (PBS, Fisher, BP3994) and then, fixed for 12 min in 1.6% formaldehyde (Sigma, F8775-25ML). Fixed cells were then washed with PBS and permeabilized for 15 min with 0.1% Triton X-100 (Sigma, T9284-100ML) in PBS. Permeabilized cells were then washed with PBS and blocked for 30 min with 1% bovine serum albumin (BSA, Fisher, BP9706-100) and 0.1% Tween-20 (Millipore, 655204-100ML) in PBS. Following blocking, cells were incubated with α-FLAG-FITC antibodies (Sigma, F4049-.2MG) diluted in blocking buffer (1% BSA and 0.1% Tween-20 PBS) at a final concentration of 1 μg/mL for 1 h at room temperature. Cells were washed with blocking buffer and analyzed using a Sony SA3800 flow cytometer.

eGFP Disruption Assays. The GFP-PEST HEK293T reporter cell line was generated via a lentiviral integration as described above and previously.[66] Briefly, HEK293T cells were transduced with lentivirus expressing an eGFP-PEST reporter construct under the EFS promoter at a MOI of 10.0. Cells with robust GFP expression were sorted on a MA900 and banked. eGFP HEK293T reporter cells were seeded into 24 well plates and transfected at 60−70% confluency the next day according to the manufacturer's protocol with lipofectamine 3000 (ThermoFisher, L3000015) using 375 ng of indicated Cas plasmids and 125 ng indicated gRNAs. Cells were analyzed 3 days post-transfection using a SA3800 flow cytometer.

TIDE Assay. DNA was isolated from the transfected cell 72 h post-transfection using a DNeasy Blood & Tissue kit (Qiagen, 69506). PCR was performed using 50 ng of extracted DNA, primers specific for the targeted *EMX1* locus, andQ5 polymerase (NEB, M0491S) following manufacturer's instructions. PCR products were then purified (Qiagen, 28106) and 100 ng of PCR products were sequenced via Sanger sequencing (Eurofins). Sequencing data was then processed using the TIDE web tool (http://tide.nki.nl).[38] Predicted Sp gRNA nuclease activities using Azimuth 2 algorithm are shown in Table S2.

Reverse-Transcription Quantitative PCR and Quantitative PCR. RNA was isolated from transfected cells using a RNeasy Plus mini kit (Qiagen, 74136) and 1 μg of purified RNA was used as a template for cDNA synthesis (Bio-Rad, 1725038). Real-time quantitative PCR (qPCR) was performed using Luna qPCR Master Mix (NEB, M3003E) and a CFX96 Real-Time PCR Detection System with a C1000 Thermal Cycler (Bio-Rad, 1855195). Baselines were subtracted using the baseline subtraction curve fit analysis mode and thresholds were automatically calculated using the Bio-Rad CFX Manager software version 2.1. Results are expressed as the fold change above mock transfected control cells after normalization to *GAPDH* expression using the $\Delta\Delta C_t$ method. Quantification of plasmid transfection efficiency was performed by creating standard curve serial dilutions of previously reported plasmid (NMS-dCas9-VP64)[19] containing a WPRE. Results were fitted to the standard curve to calculate the number of plasmids transfected, then normalized to *GAPDH*. All qPCR primers and conditions are listed in Table S3.

CRISPRa and CRISPRi Assay. The CRISPRa and CRISPRi reporter cell lines were generated using lentiviral

https://doi.org/10.1021/acssynbio.2c00156
ACS Synth. Biol. 2022, 11, 3239−3250

integration as previously described.[66] Briefly, HEK293T cells were transduced with lentivirus expressing an eGFP reporter under the miniCMV promoter at an MOI of 10.0 for CRISPRa experiments, or under an EFS promoter at an MOI of 10.0 for CRISPRi experiments, similar to previous designs.[67,68] Subsets of the populations displaying robust eGFP expression were sorted by selecting approximately 10% of the total average fluorescent population using a Sony MA900 Cell Sorter. HEK293T CRISPRa or CRISPRi reporter cells were seeded into 24 well plates and transfected at 60−70% confluency the next day according to the manufacturer's protocol with lipofectamine 3000 (ThermoFisher, L3000015) using 375 ng of indicated Cas plasmids and 125 ng associated gRNAs (Table S1). The eGFP intensity was analyzed 3 days post-transfection using a Sony SA3800 flow cytometer and compared to a non-targeting protospacer control.[69]

Statistical Analysis. Data was analyzed using Student's *t*-test. Alternative statistical analyses are presented in the source data file, along with all other source data.

■ ASSOCIATED CONTENT

Supporting Information

The Supporting Information is available free of charge at https://pubs.acs.org/doi/10.1021/acssynbio.2c00156.

Protospacer sequences, predicted nuclease efficiency, qPCR primer sequences, Cas, CRISPRi and CRISPRa fusion protein amino acid sequences, phylogenetic topologies, protein levels of Cas enzymes, RT-qPCR cycle, respective gRNA target sites, Cas variant genome editing efficacy, schematics of target sites, relative efficacy, and expression levels (PDF)

Source data file (XLSX)

■ AUTHOR INFORMATION

Corresponding Author

Isaac B. Hilton − *Department of BioSciences, Rice University, Houston, Texas 77005, United States; Department of Bioengineering, Rice University, Houston, Texas 77005, United States;* orcid.org/0000-0002-3064-8532; Email: isaac.hilton@rice.edu

Authors

Mario Escobar − *Department of BioSciences, Rice University, Houston, Texas 77005, United States;* orcid.org/0000-0003-2262-7800

Jing Li − *Department of Bioengineering, Rice University, Houston, Texas 77005, United States*

Aditi Patel − *Department of BioSciences, Rice University, Houston, Texas 77005, United States*

Shizhe Liu − *Department of BioSciences, Rice University, Houston, Texas 77005, United States*

Qi Xu − *Department of Bioengineering, Rice University, Houston, Texas 77005, United States;* orcid.org/0000-0003-4124-1364

Complete contact information is available at: https://pubs.acs.org/10.1021/acssynbio.2c00156

Author Contributions

M.E. and J.L. contributed equally to this work. M.E., J.L., and I.B.H. designed experiments and analyzed the data. M.E., J.L., A.P., S.L., and Q.X. performed experiments. M.E., J.L., and I.B.H. wrote the paper with input from all authors.

Notes

The authors declare the following competing financial interest(s): I.B.H. has filed patent applications related to CRISPR technologies for genome engineering. The remaining authors declare no competing interests.

■ ACKNOWLEDGMENTS

The authors thank all members of the Hilton laboratory for helpful discussions and feedback. This work was supported by the Cancer Prevention & Research Institute of Texas (CPRIT; RR170030 to I.B.H.), the National Institute of General Medical Sciences (R35GM143532 to I.B.H.), and the National Institute of Biomedical Imaging and Bioengineering (R21EB030772 to I.B.H.). M.E. is supported by the American Heart Association (917025/Escobar/2022).

■ ABBREVIATIONS

CRISPR, clustered regularly interspaced short palindromic repeats; Cas, CRISPR associated protein; CRISPRi, CRISPR inhibition; CRISPRa, CRISPR activation; PAM, Protospacer adjacent motif; gRNA, guide RNA; eGFP, enhanced green fluorescent protein; KRAB, Krüppel-associated box; NLS, nuclear localization sequence; EFS, EF1α shortened promoter; Indels, insertions and deletions; WT, wild type; dCas, nuclease-deactivated Cas; TSS, transcription start site; MOI, multiplicity of infection; VPR, VP64-p65-Rta; miniCMV, mini Cytomegalovirus immediate early promoter; MUSCLE, multiple sequence comparison by log-expectation; PCR, polymerase chain reaction; FBS, fetal bovine serum; PVDF, polyvinylidene fluoride; qRT-PCR, quantitative reverse-transcription quantitative PCR; HRP, Horseradish peroxidase

■ REFERENCES

(1) Makarova, K. S.; Wolf, Y. I.; Alkhnbashi, O. S.; Costa, F.; Shah, S. A.; Saunders, S. J.; Barrangou, R.; Brouns, S. J.; Charpentier, E.; Haft, D. H.; Horvath, P.; Moineau, S.; Mojica, F. J.; Terns, R. M.; Terns, M. P.; White, M. F.; Yakunin, A. F.; Garrett, R. A.; van der Oost, J.; Backofen, R.; Koonin, E. V. An updated evolutionary classification of CRISPR-Cas systems. *Nat. Rev. Microbiol.* **2015**, *13*, 722−736.

(2) Makarova, K. S.; Wolf, Y. I.; Iranzo, J.; Shmakov, S. A.; Alkhnbashi, O. S.; Brouns, S. J. J.; Charpentier, E.; Cheng, D.; Haft, D. H.; Horvath, P.; Moineau, S.; Mojica, F. J. M.; Scott, D.; Shah, S. A.; Siksnys, V.; Terns, M. P.; Venclovas, C.; White, M. F.; Yakunin, A. F.; Yan, W.; Zhang, F.; Garrett, R. A.; Backofen, R.; van der Oost, J.; Barrangou, R.; Koonin, E. V. Evolutionary classification of CRISPR-Cas systems: a burst of class 2 and derived variants. *Nat. Rev. Microbiol.* **2020**, *18*, 67−83.

(3) Jinek, M.; Chylinski, K.; Fonfara, I.; Hauer, M.; Doudna, J. A.; Charpentier, E. A programmable dual-RNA-guided DNA endonuclease in adaptive bacterial immunity. *Science* **2012**, *337*, 816−821.

(4) Cong, L.; Ran, F. A.; Cox, D.; Lin, S.; Barretto, R.; Habib, N.; Hsu, P. D.; Wu, X.; Jiang, W.; Marraffini, L. A.; Zhang, F. Multiplex genome engineering using CRISPR/Cas systems. *Science* **2013**, *339*, 819−823.

(5) Mali, P.; Yang, L.; Esvelt, K. M.; Aach, J.; Guell, M.; DiCarlo, J. E.; Norville, J. E.; Church, G. M. RNA-guided human genome engineering via Cas9. *Science* **2013**, *339*, 823−826.

(6) Zetsche, B.; Gootenberg, J. S.; Abudayyeh, O. O.; Slaymaker, I. M.; Makarova, K. S.; Essletzbichler, P.; Volz, S. E.; Joung, J.; van der Oost, J.; Regev, A.; Koonin, E. V.; Zhang, F. Cpf1 is a single RNA-guided endonuclease of a class 2 CRISPR-Cas system. *Cell* **2015**, *163*, 759−771.

(7) Liu, J. J.; Orlova, N.; Oakes, B. L.; Ma, E.; Spinner, H. B.; Baney, K. L. M.; Chuck, J.; Tan, D.; Knott, G. J.; Harrington, L. B.; Al-

Shayeb, B.; Wagner, A.; Brötzmann, J.; Staahl, B. T.; Taylor, K. L.; Desmarais, J.; Nogales, E.; Doudna, J. A. CasX enzymes comprise a distinct family of RNA-guided genome editors. *Nature* **2019**, *566*, 218−223.
(8) Strecker, J.; Jones, S.; Koopal, B.; Schmid-Burgk, J.; Zetsche, B.; Gao, L.; Makarova, K. S.; Koonin, E. V.; Zhang, F. Engineering of CRISPR-Cas12b for human genome editing. *Nat. Commun.* **2019**, *10*, 212.
(9) Pausch, P.; Al-Shayeb, B.; Bisom-Rapp, E.; Tsuchida, C. A.; Li, Z.; Cress, B. F.; Knott, G. J.; Jacobsen, S. E.; Banfield, J. F.; Doudna, J. A. CRISPR-CasPhi from huge phages is a hypercompact genome editor. *Science* **2020**, *369*, 333−337.
(10) Wu, Z.; Zhang, Y.; Yu, H.; Pan, D.; Wang, Y.; Wang, Y.; Li, F.; Liu, C.; Nan, H.; Chen, W.; Ji, Q. Programmed genome editing by a miniature CRISPR-Cas12f nuclease. *Nat. Chem. Biol.* **2021**, *17*, 1132−1138.
(11) Kim, D. Y.; Lee, J. M.; Moon, S. B.; Chin, H. J.; Park, S.; Lim, Y.; Kim, D.; Koo, T.; Ko, J. H.; Kim, Y. S. Efficient CRISPR editing with a hypercompact Cas12f1 and engineered guide RNAs delivered by adeno-associated virus. *Nat. Biotechnol.* **2022**, *40*, 94−102.
(12) Gilbert, L. A.; Larson, M. H.; Morsut, L.; Liu, Z.; Brar, G. A.; Torres, S. E.; Stern-Ginossar, N.; Brandman, O.; Whitehead, E. H.; Doudna, J. A.; Lim, W. A.; Weissman, J. S.; Qi, L. S. CRISPR-mediated modular RNA-guided regulation of transcription in eukaryotes. *Cell* **2013**, *154*, 442−451.
(13) Qi, L. S.; Larson, M. H.; Gilbert, L. A.; Doudna, J. A.; Weissman, J. S.; Arkin, A. P.; Lim, W. A. Repurposing CRISPR as an RNA-guided platform for sequence-specific control of gene expression. *Cell* **2013**, *152*, 1173−1183.
(14) Chavez, A.; Scheiman, J.; Vora, S.; Pruitt, B. W.; Tuttle, M.; P R Iyer, P. R. I.; Lin, S.; Kiani, S.; Guzman, C. D.; Wiegand, D. J.; Ter-Ovanesyan, D.; Braff, J. L.; Davidsohn, N.; Housden, B. E.; Perrimon, N.; Weiss, R.; Aach, J.; Collins, J. J.; Church, G. M. Highly efficient Cas9-mediated transcriptional programming. *Nat. Methods* **2015**, *12*, 326−328.
(15) Hilton, I. B.; D'Ippolito, A. M.; Vockley, C. M.; Thakore, P. I.; Crawford, G. E.; Reddy, T. E.; Gersbach, C. A. Epigenome editing by a CRISPR-Cas9-based acetyltransferase activates genes from promoters and enhancers. *Nat. Biotechnol.* **2015**, *33*, 510−517.
(16) Goell, J. H.; Hilton, I. B. CRISPR/Cas-Based Epigenome Editing: Advances, Applications, and Clinical Utility. *Trends Biotechnol.* **2021**, *39*, 678−691.
(17) Li, J.; Mahata, B.; Escobar, M.; Goell, J.; Wang, K.; Khemka, P.; Hilton, I. B. Programmable human histone phosphorylation and gene activation using a CRISPR/Cas9-based chromatin kinase. *Nat. Commun.* **2021**, *12*, 896.
(18) Wang, K.; Escobar, M.; Li, J.; Mahata, B.; Goell, J.; Shah, S.; Cluck, M.; Hilton, I. B. Systematic comparison of CRISPR-based transcriptional activators uncovers gene-regulatory features of enhancer-promoter interactions. *Nucleic Acids Res.* **2022**, *50*, 7842.
(19) Mahata, B.; Li, J.; Cabrera, A.; Brenner, D. A.; Guerra-Resendez, R. S.; Goell, J.; Wang, K.; Escobar, M.; Guo, Y.; Parthasarathy, A. K.; Hilton, I. B. Compact engineered human transactivation modules enable potent and versatile synthetic transcriptional control. **2022**. bioRxiv:2003.2021.485228.
(20) Chew, W. L.; Tabebordbar, M.; Cheng, J. K.; Mali, P.; Wu, E. Y.; Ng, A. H.; Zhu, K.; Wagers, A. J.; Church, G. M. A multifunctional AAV-CRISPR-Cas9 and its host response. *Nat. Methods* **2016**, *13*, 868−874.
(21) Cradick, T. J.; Fine, E. J.; Antico, C. J.; Bao, G. CRISPR/Cas9 systems targeting beta-globin and CCR5 genes have substantial off-target activity. *Nucleic Acids Res.* **2013**, *41*, 9584−9592.
(22) Dever, D. P.; Bak, R. O.; Reinisch, A.; Camarena, J.; Washington, G.; Nicolas, C. E.; Pavel-Dinu, M.; Saxena, N.; Wilkens, A. B.; Mantri, S.; Uchida, N.; Hendel, A.; Narla, A.; Majeti, R.; Weinberg, K. I.; Porteus, M. H. CRISPR/Cas9 beta-globin gene targeting in human haematopoietic stem cells. *Nature* **2016**, *539*, 384−389.
(23) Chen, J. S.; Dagdas, Y. S.; Kleinstiver, B. P.; Welch, M. M.; Sousa, A. A.; Harrington, L. B.; Sternberg, S. H.; Joung, J. K.; Yildiz, A.; Doudna, J. A. Enhanced proofreading governs CRISPR-Cas9 targeting accuracy. *Nature* **2017**, *550*, 407−410.
(24) Kleinstiver, B. P.; Pattanayak, V.; Prew, M. S.; Tsai, S. Q.; Nguyen, N. T.; Zheng, Z.; Joung, J. K. High-fidelity CRISPR-Cas9 nucleases with no detectable genome-wide off-target effects. *Nature* **2016**, *529*, 490−495.
(25) Vakulskas, C. A.; Dever, D. P.; Rettig, G. R.; Turk, R.; Jacobi, A. M.; Collingwood, M. A.; Bode, N. M.; McNeill, M. S.; Yan, S.; Camarena, J.; Lee, C. M.; Park, S. H.; Wiebking, V.; Bak, R. O.; Gomez-Ospina, N.; Pavel-Dinu, M.; Sun, W.; Bao, G.; Porteus, M. H.; Behlke, M. A. A high-fidelity Cas9 mutant delivered as a ribonucleoprotein complex enables efficient gene editing in human hematopoietic stem and progenitor cells. *Nat. Med.* **2018**, *24*, 1216−1224.
(26) Walton, R. T.; Christie, K. A.; Whittaker, M. N.; Kleinstiver, B. P. Unconstrained genome targeting with near-PAMless engineered CRISPR-Cas9 variants. *Science* **2020**, *368*, 290−296.
(27) Kleinstiver, B. P.; Prew, M. S.; Tsai, S. Q.; Topkar, V. V.; Nguyen, N. T.; Zheng, Z.; Gonzales, A. P.; Li, Z.; Peterson, R. T.; Yeh, J. R.; Aryee, M. J.; Joung, J. K. Engineered CRISPR-Cas9 nucleases with altered PAM specificities. *Nature* **2015**, *523*, 481−485.
(28) Nishimasu, H.; Shi, X.; Ishiguro, S.; Gao, L.; Hirano, S.; Okazaki, S.; Noda, T.; Abudayyeh, O. O.; Gootenberg, J. S.; Mori, H.; Oura, S.; Holmes, B.; Tanaka, M.; Seki, M.; Hirano, H.; Aburatani, H.; Ishitani, R.; Ikawa, M.; Yachie, N.; Zhang, F.; Nureki, O. Engineered CRISPR-Cas9 nuclease with expanded targeting space. *Science* **2018**, *361*, 1259−1262.
(29) Hu, J. H.; Miller, S. M.; Geurts, M. H.; Tang, W.; Chen, L.; Sun, N.; Zeina, C. M.; Gao, X.; Rees, H. A.; Lin, Z.; Liu, D. R. Evolved Cas9 variants with broad PAM compatibility and high DNA specificity. *Nature* **2018**, *556*, 57−63.
(30) Ran, F. A.; Cong, L.; Yan, W. X.; Scott, D. A.; Gootenberg, J. S.; Kriz, A. J.; Zetsche, B.; Shalem, O.; Wu, X.; Makarova, K. S.; Koonin, E. V.; Sharp, P. A.; Zhang, F. In vivo genome editing using Staphylococcus aureus Cas9. *Nature* **2015**, *520*, 186−191.
(31) Hou, Z.; Zhang, Y.; Propson, N. E.; Howden, S. E.; Chu, L. F.; Sontheimer, E. J.; Thomson, J. A. Efficient genome engineering in human pluripotent stem cells using Cas9 from Neisseria meningitidis. *Proc. Natl. Acad. Sci. U.S.A.* **2013**, *110*, 15644−15649.
(32) Esvelt, K. M.; Mali, P.; Braff, J. L.; Moosburner, M.; Yaung, S. J.; Church, G. M. Orthogonal Cas9 proteins for RNA-guided gene regulation and editing. *Nat. Methods* **2013**, *10*, 1116−1121.
(33) Kim, E.; Koo, T.; Park, S. W.; Kim, D.; Kim, K.; Cho, H. Y.; Song, D. W.; Lee, K. J.; Jung, M. H.; Kim, S.; Kim, J. H.; Kim, J. H.; Kim, J. S. In vivo genome editing with a small Cas9 orthologue derived from Campylobacter jejuni. *Nat. Commun.* **2017**, *8*, 14500.
(34) Tong, B.; Dong, H.; Cui, Y.; Jiang, P.; Jin, Z.; Zhang, D. The Versatile Type V CRISPR Effectors and Their Application Prospects. *Front. Cell. Dev. Biol.* **2020**, *8*, 622103.
(35) Fu, Y.; Foden, J. A.; Khayter, C.; Maeder, M. L.; Reyon, D.; Joung, J. K.; Sander, J. D. High-frequency off-target mutagenesis induced by CRISPR-Cas nucleases in human cells. *Nat. Biotechnol.* **2013**, *31*, 822−826.
(36) Maji, B.; Gangopadhyay, S. A.; Lee, M.; Shi, M.; Wu, P.; Heler, R.; Mok, B.; Lim, D.; Siriwardena, S. U.; Paul, B.; Dančík, V.; Vetere, A.; Mesleh, M. F.; Marraffini, L. A.; Liu, D. R.; Clemons, P. A.; Wagner, B. K.; Choudhary, A. A High-Throughput Platform to Identify Small-Molecule Inhibitors of CRISPR-Cas9. *Cell* **2019**, *177*, 1067−1079.
(37) Xie, H.; Tang, L.; He, X.; Liu, X.; Zhou, C.; Liu, J.; Ge, X.; Li, J.; Liu, C.; Zhao, J.; Qu, J.; Song, Z.; Gu, F. SaCas9 Requires 5'-NNGRRT-3' PAM for Sufficient Cleavage and Possesses Higher Cleavage Activity than SpCas9 or FnCpf1 in Human Cells. *Biotechnol. J.* **2018**, *13*, No. e1700561.
(38) Brinkman, E. K.; Chen, T.; Amendola, M.; van Steensel, B. Easy quantitative assessment of genome editing by sequence trace decomposition. *Nucleic Acids Res.* **2014**, *42*, No. e168.

https://doi.org/10.1021/acssynbio.2c00156
ACS Synth. Biol. 2022, 11, 3239−3250

(39) Thakore, P. I.; Black, J. B.; Hilton, I. B.; Gersbach, C. A. Editing the epigenome: technologies for programmable transcription and epigenetic modulation. *Nat. Methods* **2016**, *13*, 127−137.
(40) Konermann, S.; Brigham, M. D.; Trevino, A. E.; Joung, J.; Abudayyeh, O. O.; Barcena, C.; Hsu, P. D.; Habib, N.; Gootenberg, J. S.; Nishimasu, H.; Nureki, O.; Zhang, F. Genome-scale transcriptional activation by an engineered CRISPR-Cas9 complex. *Nature* **2015**, *517*, 583−588.
(41) Perez-Pinera, P.; Kocak, D. D.; Vockley, C. M.; Adler, A. F.; Kabadi, A. M.; Polstein, L. R.; Thakore, P. I.; Glass, K. A.; Ousterout, D. G.; Leong, K. W.; Guilak, F.; Crawford, G. E.; Reddy, T. E.; Gersbach, C. A. RNA-guided gene activation by CRISPR-Cas9-based transcription factors. *Nat. Methods* **2013**, *10*, 973−976.
(42) Morita, S.; Noguchi, H.; Horii, T.; Nakabayashi, K.; Kimura, M.; Okamura, K.; Sakai, A.; Nakashima, H.; Hata, K.; Nakashima, K.; Hatada, I. Targeted DNA demethylation in vivo using dCas9-peptide repeat and scFv-TET1 catalytic domain fusions. *Nat. Biotechnol.* **2016**, *34*, 1060−1065.
(43) Campa, C. C.; Weisbach, N. R.; Santinha, A. J.; Incarnato, D.; Platt, R. J. Multiplexed genome engineering by Cas12a and CRISPR arrays encoded on single transcripts. *Nat. Methods* **2019**, *16*, 887−893.
(44) Umkehrer, C.; Holstein, F.; Formenti, L.; Jude, J.; Froussios, K.; Neumann, T.; Cronin, S. M.; Haas, L.; Lipp, J. J.; Burkard, T. R.; Fellner, M.; Wiesner, T.; Zuber, J.; Obenauf, A. C. Isolating live cell clones from barcoded populations using CRISPRa-inducible reporters. *Nat. Biotechnol.* **2021**, *39*, 174−178.
(45) Schmidt, R.; Steinhart, Z.; Layeghi, M.; Freimer, J. W.; Bueno, R.; Nguyen, V. Q.; Blaeschke, F.; Ye, C. J.; Marson, A. CRISPR activation and interference screens decode stimulation responses in primary human T cells. *Science* **2022**, *375*, No. eabj4008.
(46) Thakore, P. I.; D'Ippolito, A. M.; Song, L.; Safi, A.; Shivakumar, N. K.; Kabadi, A. M.; Reddy, T. E.; Crawford, G. E.; Gersbach, C. A. Highly specific epigenome editing by CRISPR-Cas9 repressors for silencing of distal regulatory elements. *Nat. Methods* **2015**, *12*, 1143−1149.
(47) Concordet, J. P.; Haeussler, M. CRISPOR: intuitive guide selection for CRISPR/Cas9 genome editing experiments and screens. *Nucleic Acids Res.* **2018**, *46*, W242−W245.
(48) Haeussler, M.; Schönig, K.; Eckert, H.; Eschstruth, A.; Mianné, J.; Renaud, J. B.; Schneider-Maunoury, S.; Shkumatava, A.; Teboul, L.; Kent, J.; Joly, J. S.; Concordet, J. P. Evaluation of off-target and on-target scoring algorithms and integration into the guide RNA selection tool CRISPOR. *Genome Biol.* **2016**, *17*, 148.
(49) Nuñez, J. K.; Chen, J.; Pommier, G. C.; Cogan, J. Z.; Replogle, J. M.; Adriaens, C.; Ramadoss, G. N.; Shi, Q.; Hung, K. L.; Samelson, A. J.; Pogson, A. N.; Kim, J. Y. S.; Chung, A.; Leonetti, M. D.; Chang, H. Y.; Kampmann, M.; Bernstein, B. E.; Hovestadt, V.; Gilbert, L. A.; Weissman, J. S. Genome-wide programmable transcriptional memory by CRISPR-based epigenome editing. *Cell* **2021**, *184*, 2503−2519.
(50) Yeo, N. C.; Chavez, A.; Lance-Byrne, A.; Chan, Y.; Menn, D.; Milanova, D.; Kuo, C. C.; Guo, X.; Sharma, S.; Tung, A.; Cecchi, R. J.; Tuttle, M.; Pradhan, S.; Lim, E. T.; Davidsohn, N.; Ebrahimkhani, M. R.; Collins, J. J.; Lewis, N. E.; Kiani, S.; Church, G. M. An enhanced CRISPR repressor for targeted mammalian gene regulation. *Nat. Methods* **2018**, *15*, 611−616.
(51) Xu, X.; Chemparathy, A.; Zeng, L.; Kempton, H. R.; Shang, S.; Nakamura, M.; Qi, L. S. Engineered miniature CRISPR-Cas system for mammalian genome regulation and editing. *Mol. Cell* **2021**, *81*, 4333−4345.
(52) Dong, D.; Ren, K.; Qiu, X.; Zheng, J.; Guo, M.; Guan, X.; Liu, H.; Li, N.; Zhang, B.; Yang, D.; Ma, C.; Wang, S.; Wu, D.; Ma, Y.; Fan, S.; Wang, J.; Gao, N.; Huang, Z. The crystal structure of Cpf1 in complex with CRISPR RNA. *Nature* **2016**, *532*, 522−526.
(53) Bin Moon, S.; Lee, J. M.; Kang, J. G.; Lee, N. E.; Ha, D. I.; Kim, D. Y.; Kim, S. H.; Yoo, K.; Kim, D.; Ko, J. H.; Kim, Y. S. Highly efficient genome editing by CRISPR-Cpf1 using CRISPR RNA with a uridinylate-rich 3'-overhang. *Nat. Commun.* **2018**, *9*, 3651.
(54) Wright, A. V.; Sternberg, S. H.; Taylor, D. W.; Staahl, B. T.; Bardales, J. A.; Kornfeld, J. E.; Doudna, J. A. Rational design of a split-Cas9 enzyme complex. *Proc. Natl. Acad. Sci. U.S.A.* **2015**, *112*, 2984−2989.
(55) Ling, X.; Chang, L.; Chen, H.; Gao, X.; Yin, J.; Zuo, Y.; Huang, Y.; Zhang, B.; Hu, J.; Liu, T. Improving the efficiency of CRISPR-Cas12a-based genome editing with site-specific covalent Cas12a-crRNA conjugates. *Mol. Cell* **2021**, *81*, 4747−4756.
(56) Kim, D.; Bae, S.; Park, J.; Kim, E.; Kim, S.; Yu, H. R.; Hwang, J.; Kim, J. I.; Kim, J. S. Digenome-seq: genome-wide profiling of CRISPR-Cas9 off-target effects in human cells. *Nat. Methods* **2015**, *12*, 231.
(57) Tsai, S. Q.; Zheng, Z.; Nguyen, N. T.; Liebers, M.; Topkar, V. V.; Thapar, V.; Wyvekens, N.; Khayter, C.; Iafrate, A. J.; Le, L. P.; Aryee, M. J.; Joung, J. K. GUIDE-seq enables genome-wide profiling of off-target cleavage by CRISPR-Cas nucleases. *Nat. Biotechnol.* **2015**, *33*, 187−197.
(58) Kleinstiver, B. P.; Tsai, S. Q.; Prew, M. S.; Nguyen, N. T.; Welch, M. M.; Lopez, J. M.; McCaw, Z. R.; Aryee, M. J.; Joung, J. K. Genome-wide specificities of CRISPR-Cas Cpf1 nucleases in human cells. *Nat. Biotechnol.* **2016**, *34*, 869−874.
(59) Kleinstiver, B. P.; Sousa, A. A.; Walton, R. T.; Tak, Y. E.; Hsu, J. Y.; Clement, K.; Welch, M. M.; Horng, J. E.; Malagon-Lopez, J.; Scarfò, I.; Maus, M. V.; Pinello, L.; Aryee, M. J.; Joung, J. K. Engineered CRISPR-Cas12a variants with increased activities and improved targeting ranges for gene, epigenetic and base editing. *Nat. Biotechnol.* **2019**, *37*, 276−282.
(60) Liu, P.; Luk, K.; Shin, M.; Idrizi, F.; Kwok, S.; Roscoe, B.; Mintzer, E.; Suresh, S.; Morrison, K.; Frazão, J. B.; Bolukbasi, M. F.; Ponnienselvan, K.; Luban, J.; Zhu, L. J.; Lawson, N. D.; Wolfe, S. A. Enhanced Cas12a editing in mammalian cells and zebrafish. *Nucleic Acids Res.* **2019**, *47*, 4169−4180.
(61) Jones, S. K., Jr.; Hawkins, J. A.; Johnson, N. V.; Jung, C.; Hu, K.; Rybarski, J. R.; Chen, J. S.; Doudna, J. A.; Press, W. H.; Finkelstein, I. J. Massively parallel kinetic profiling of natural and engineered CRISPR nucleases. *Nat. Biotechnol.* **2021**, *39*, 84−93.
(62) Li, B.; Zhao, W.; Luo, X.; Zhang, X.; Li, C.; Zeng, C.; Dong, Y. Engineering CRISPR-Cpf1 crRNAs and mRNAs to maximize genome editing efficiency. *Nat. Biomed. Eng.* **2017**, *1*, 0066.
(63) Kocak, D. D.; Josephs, E. A.; Bhandarkar, V.; Adkar, S. S.; Kwon, J. B.; Gersbach, C. A. Increasing the specificity of CRISPR systems with engineered RNA secondary structures. *Nat. Biotechnol.* **2019**, *37*, 657−666.
(64) Madeira, F.; Park, Y. M.; Lee, J.; Buso, N.; Gur, T.; Madhusoodanan, N.; Basutkar, P.; Tivey, A. R. N.; Potter, S. C.; Finn, R. D.; Lopez, R. The EMBL-EBI search and sequence analysis tools APIs in 2019. *Nucleic Acids Res.* **2019**, *47*, W636−W641.
(65) Stecher, G.; Tamura, K.; Kumar, S. Molecular Evolutionary Genetics Analysis (MEGA) for macOS. *Mol. Biol. Evol.* **2020**, *37*, 1237−1239.
(66) Richardson, C. D.; Ray, G. J.; DeWitt, M. A.; Curie, G. L.; Corn, J. E. Enhancing homology-directed genome editing by catalytically active and inactive CRISPR-Cas9 using asymmetric donor DNA. *Nat. Biotechnol.* **2016**, *34*, 339−344.
(67) Tycko, J.; DelRosso, N.; Hess, G. T.; Aradhana; Banerjee, A.; Mukund, M. V.; Van, B. K.; Ego, D.; Yao, K.; Spees, P.; Suzuki, G. K.; Marinov, A.; Kundaje, M. C.; Bassik, L.; Bintu, L. High-Throughput Discovery and Characterization of Human Transcriptional Effectors. *Cell* **2020**, *183*, 2020−2035.
(68) Van, M. V.; Fujimori, T.; Bintu, L. Nanobody-mediated control of gene expression and epigenetic memory. *Nat. Commun.* **2021**, *12*, 537.
(69) Ruan, G. X.; Barry, E.; Yu, D.; Lukason, M.; Cheng, S. H.; Scaria, A. CRISPR/Cas9-Mediated Genome Editing as a Therapeutic Approach for Leber Congenital Amaurosis 10. *Mol. Ther.* **2017**, *25*, 331−341.

https://doi.org/10.1021/acssynbio.2c00156
ACS Synth. Biol. 2022, 11, 3239−3250